The Influence of Processing Parameters on the Properties of Melt-Spun Polypropylene Hollow Fibers

ANNE DE ROVERE, BRIAN P. GRADY, ROBERT L. SHAMBAUGH

The University of Oklahoma, School of Chemical Engineering and Materials Science, Norman, Oklahoma 73019

Received 12 February 2001; accepted 5 June 2001

ABSTRACT: Isotactic polypropylene hollow fibers were produced by melt spinning. Spinning speeds up to 1880 m/min were used, and sample hollowness (percentage void in cross section) ranged from 0 to 69%. The fiber samples were characterized using dynamic mechanical analysis, birefringence, tensile testing, and differential scanning calorimetry. The hollow fibers were found to have higher crystallinity, orientation, and strength than the analogous solid fibers. In general, the polymer orientation in a hollow fiber was larger than the orientation in a solid fiber, even when the spinning speed for the latter was much larger. For a fixed outer diameter, increasing the hollowness improved fiber properties. However, as hollowness was further increased, fiber properties declined slightly. At a given percentage hollowness, increased spinning speed increased modulus and tenacity. © 2002 John Wiley & Sons, Inc. J Appl Polym Sci 83: 1759–1772, 2002

Key words: polypropylene; fiber; spinning; hollow; modulus

INTRODUCTION

Hollow fibers have been used primarily in separation processes. Artificial kidneys are an excellent example.[1] Fibers such as those used in artificial kidneys are difficult to produce because the required filtration properties necessitate strict control of wall properties. These properties (microporous walls, asymmetric walls, etc.) require the spinning of hollow fiber membranes at relatively slow spinning speeds. For example, J. J. Kim et al.[2] produced polypropylene hollow fibers with take-up speeds as low as 76.6 cm/min, whereas J. H. Kim et al.[3] produced wet-spun fibers at speeds of only 10–35 m/min.

The rate of fiber spinning as well as any subsequent cold drawing changes the properties of a fiber dramatically. The high modulus and tensile strength of semicrystalline commercial synthetic fibers, including polypropylene, are usually caused by morphological transformations and chain-orientation procedures.[4] High-performance fibers are usually obtained when both crystallinity and orientation are increased. For example, high-strength polyester can be produced by spinning at about 3000 m/min and then post-drawing (off-line drawing) at about a 2 : 1 draw ratio. Similar polyester strengths can result from high-speed spinning at about 6000 m/min. Though the process is not commercial, extremely strong polyethylene fibers can be made by a solid-state extrusion and drawing process.[4] All these processes impart high strength and modulus to the fibers.

Melt to draw ratio, spinneret temperature, and annealing temperature are also important factors influencing a fiber's structure and performance. Kim et al.[2,5] studied the effects of cold drawing and spinning temperatures on polypropylene hollow-fiber morphology. Annealing at 60 to 140°C was found to increase fiber crystallinity without changing orientation. High melt–draw ratios

Correspondence to: R. L. Shambaugh (shambaugh@ou.edu).

Journal of Applied Polymer Science, Vol. 83, 1759–1772 (2002)

DOI 10.1002/app.10128

(1000–1250%) were found to increase the hollow-fiber orientation.[2]

Unlike the situation with hollow fiber membranes, hollow fibers can also be produced for applications where fiber wall filtration properties are not critical. The advantage of hollow fibers over solid fibers is their lower cost and lighter weight on a per outside diameter basis. In this article, we show how polymer flow rate, spinning speed, and fiber hollowness affect the morphology and mechanical properties of hollow filaments. Fiber morphology was characterized using differential scanning calorimetry (DSC) and birefringence. Mechanical properties of the fibers were evaluated by tensile tests at room temperature. Dynamic mechanical analysis (DMA) was used to (1) measure the glass transition temperature (T_g) and (2) estimate the elastic modulus as a function of temperature. At a constant outside diameter, our results show that it is possible to obtain a hollow fiber with higher strength and modulus than those of the analogous solid fiber.

EXPERIMENTAL EQUIPMENT

Fiber Production

Fina Dypro® isotactic polypropylene pellets with a melt flow rate (MFR) of 88, a weight average molecular weight of 165,000 g/mol, and a polydispersity of 4 were melted at 200°C and spun at 200°C to produce the fibers. Both hollow and solid fibers were obtained by melt extrusion using a tube-in-orifice spinneret.[6] Nitrogen gas was injected in the center of the molten filament to produce the hollow structure. Spinning with the nitrogen turned off resulted in solid filaments. All fibers were attenuated with a mechanical take-up roll that also served to collect the fibers. No fiber post-drawing was used (i.e., the fibers were "as spun").

Fiber diameters were measured under an optical microscope equipped with a micrometer eyepiece. The diameters of the solid fibers were measured from side views of the fibers. For hollow fibers, outer and inner diameters were determined from cross-sectional views obtained by microtoming the samples. A distinction needs to be made between polymer and fiber cross-sectional areas. The polymer cross-sectional area (S_p) represents the area of the polymer annulus only, whereas the fiber cross-sectional area (S_f) represents the total cross-sectional area of the fiber based on the outside diameter. Hence, S_f is larger than S_p except in the case of solid fiber, where the two are equal.

Tensile Test

A model TT-B-L Instron Tensile Tester was used to measure tensile properties. A B-load cell with a sensitivity in the range of 100–2000 g was used in all experiments. Special pneumatic grips with a working pressure of 0.138 MPa (20 psi) were used to hold the samples in place. A crosshead speed (stretching rate) of 2.54 cm/min was used for all experiments. The initial length of the sample was set at 2.2 cm. Careful attention was taken to minimize stretching of the fiber before testing and while placing the sample in the grips. The procedure followed is described in ASTM D 2101-93.

Young's modulus was calculated from the initial slope of the tensile curve. The elongation and stress at break were determined at the position of rupture. Toughness was obtained by numerically integrating the area under the stress–strain curve. Tenacity and modulus were calculated in textile units of grams per denier. Denier (den) is a textile unit based on the weight in grams of 9000 m of fiber (the lower the number, the finer the fiber). Tensile strength in pounds/inch^2 is related to grams/den by the relation[7]

$$\text{tensile strength (lb/in}^2) = 12{,}800 \times \text{specific gravity} \times \text{tenacity (g/den)} \quad (1)$$

where the specific gravity for polypropylene was assumed to be a constant 0.895.[8] Reported values were averages from three replicate tests on short fiber segments cut from the same length of fiber. The confidence intervals for a reliability of 0.95 were ±20% for tenacity, ±20% for rupture elongation, and ±15% for Young's modulus.

Commercial polypropylene fibers are available ranging in tenacity from 2–4 g/den for carpeting, 3–6 g/den for textiles, and 6–9 g/den for industrial purposes. Polypropylene fibers also differ widely in their elastic moduli, ranging from 120 g/den for well-annealed monofilaments to 25 g/den for carpet staple. For textile fibers, a mean value of 50–60 g/den is common.[7] Modulus and tenacity values for fibers in this article are lower than commercial values because no post-drawing was applied to our fibers.

Dynamic Mechanical Analysis

A solids analyzer RSA II (Rheometric Scientific, Piscataway, NJ) was operated with a nitrogen gas

Table I Dynamic Mechanical Analysis Test Sequence

	Sequence 1	Sequence 2	Sequence 3
Initial temperature (°C)	−100	−30	40
Final temperature (°C)	−30	40	200
Temperature increment (°C)	8	2	4
Soak time (sec)	6	6	6
Strain (%)	0.1	0.1	0.1

atmosphere, tensile deformation mode, and autotension. Temperature steps were used, and the test sequence is given in Table I. All samples were mounted with approximately 0.5 g of pretension before starting the test. This nominally positive (tensile) force was applied to the sample so that the instrument could maintain the sample under slight tension as the sample cools. The sample length after cooling was entered into the computer program; however, no correction was entered for the presumably smaller diameter. An initial static force of 5 g (applied at −100°C) was used to start the test. All experiments were performed with a 10-Hz frequency and a 0.1% strain.

To be sure that the initial static force was not affecting our results, the pretension applied to the fiber at −100°C was varied by ±20% around the base case of 5 g (for a 45.6-μm-diameter solid fiber). Within the error shown in Figure 1, this change of pretension affected neither the value of the modulus nor the value of the T_g. Similarly, Khanna et al.[9,10] observed that, when the pretension was increased by two orders of magnitude, there was only a 6% increase in the modulus of an experimental polymer fiber. To ascertain that measurements were conducted in the linear viscoelastic region, the strain was also varied by ±20% around the base case of 0.1%; no difference

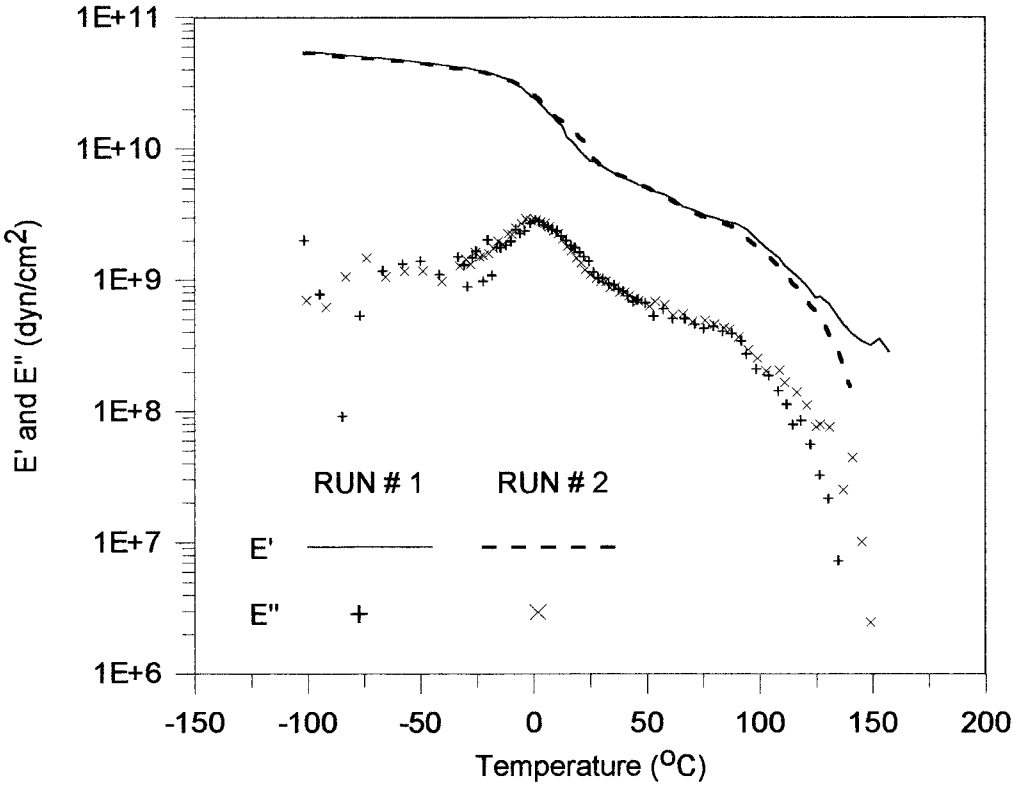

Figure 1 Storage modulus E' and loss modulus E'' as a function of temperature for two repeat runs on the same sample. Fiber outer diameter = 54.6 μm; take-up speed = 840 m/min.

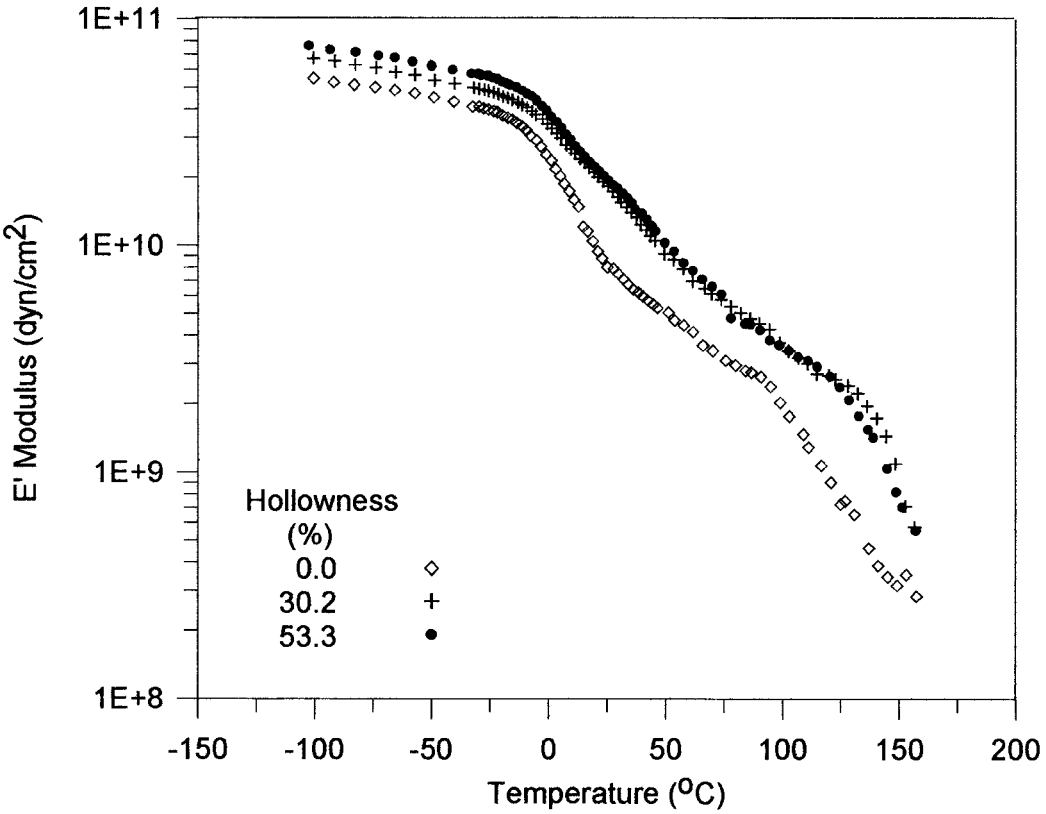

Figure 2 Storage modulus E' as a function of temperature for fibers with constant cross-sectional area and various hollowness. Polymer throughput = 1.35 g/min; take-up speed = 840 m/min.

was found in either E' (storage modulus, dyne/cm^2) or E'' (loss modulus, dyne/cm^2). Thus, the results reported in this article are characteristic of fiber properties and contain no measurable contributions from pretension or strain. Except where noted, modulus calculations were based on the polymer cross-sectional area (S_p).

To test reproducibility, two fibers segments were taken from the same fiber sample; these segments were tested under the conditions described in Table I. The sample, which was a solid filament of 45.6 μm outer diamter (OD), was spun with a spinning speed of 840 m/min. As shown in Figure 1, E' and E'' curves for these two segments are almost perfectly overlapping from -100 to 100°C; only at higher temperatures is there a slight difference between the curves. This reproducibility also illustrates that there was minimal stretching of the samples during loading.

T_g was determined from the peak of the loss modulus curves, E''. The curves were fitted with a sixth-order polynomial function, and the maximum ($dE''/dT = 0$) was used to determined T_g. Glass transition temperatures of 1.41 and -0.28°C were obtained from the two duplicate samples. As there is little difference between the two values, the reproducibility of the glass transition temperatures obtained via this method is also quite good.

Birefringence

A Nikon polarizing microscope (LabPhot2-pol, Nikon, Inc., Melville, NY) was used for measuring the birefringence of a sample. The Senarmont compensator technique was used to determine the retardation, which is the phase difference between light waves oriented parallel to and perpendicular to the stretch direction; see Gander and Schaefer.[11] According to the following formula, the retardation is proportional to the birefringence:

$$\text{birefringence} = \text{relative retardation (nm)}/\text{specimen thickness (nm)} \quad (2)$$

For solid filaments, the specimen thickness is defined as the filament diameter. For hollow fila-

Table II Fiber Properties at Constant Polymer Cross-Sectional Area[a]

Hollowness (%)	Birefringence	T_g (°C)[b]	T_m (°C)[c]	Crystallinity (%)[c]
0	0.00372	−0.3	161	39.6
30.2	0.00587	0.8	164	50.3
53.3	0.00738	1.1	164	50.2

[a] The polymer throughput was 1.35 g/min, and the take-up speed was 840 m/min.
[b] From dynamic mechanical analysis measurements.
[c] From differential scanning calorimetry measurements.

ments, the thickness is defined as the difference between the outer and inner diameters. In other words, specimen thickness is two times the fiber wall thickness, as the refracted light goes through the fiber wall twice. The birefringence measurement gives the overall orientation of both the crystalline and amorphous regions.

Differential Scanning Calorimetry

A differential scanning calorimeter (DSC-2, Perkin-Elmer, Shelton, CT) was used to measure the heat of fusion of a polymer, ΔH_f (J/g), and the melting temperature T_m. On the basis of the results of Bershtein and Egorov,[12] a rather slow heating rate of 1.25°C/min was selected for our tests. Bershtein and Egorov studied the effect of heating rate on endothermic melting peaks; they showed that the lower the heating rate, the more accurate the melting point. According to Bershtein and Egorov, the melting point measured at a 1.25°C/min rate is less than a degree different than what would be measured at an infinitely slow heating rate. Also, at this low heating rate, more resolved peak shapes are developed. The temperature scale was calibrated with an indium standard (T_m = 156.6°C) and a tin standard (T_m = 231.8°C).

The preparation of fiber samples for reproducible results presents special problems for the DSC analysis of polymer fibers. To avoid any heat-transfer limitations between the fibers and the aluminum pan, polypropylene fibers were cut into pieces approximately 0.5 mm in length, using a fresh razor blade for each sample. Special attention was taken to avoid stretching the fibers. Sample weights of 1.0–4.0 mg were determined

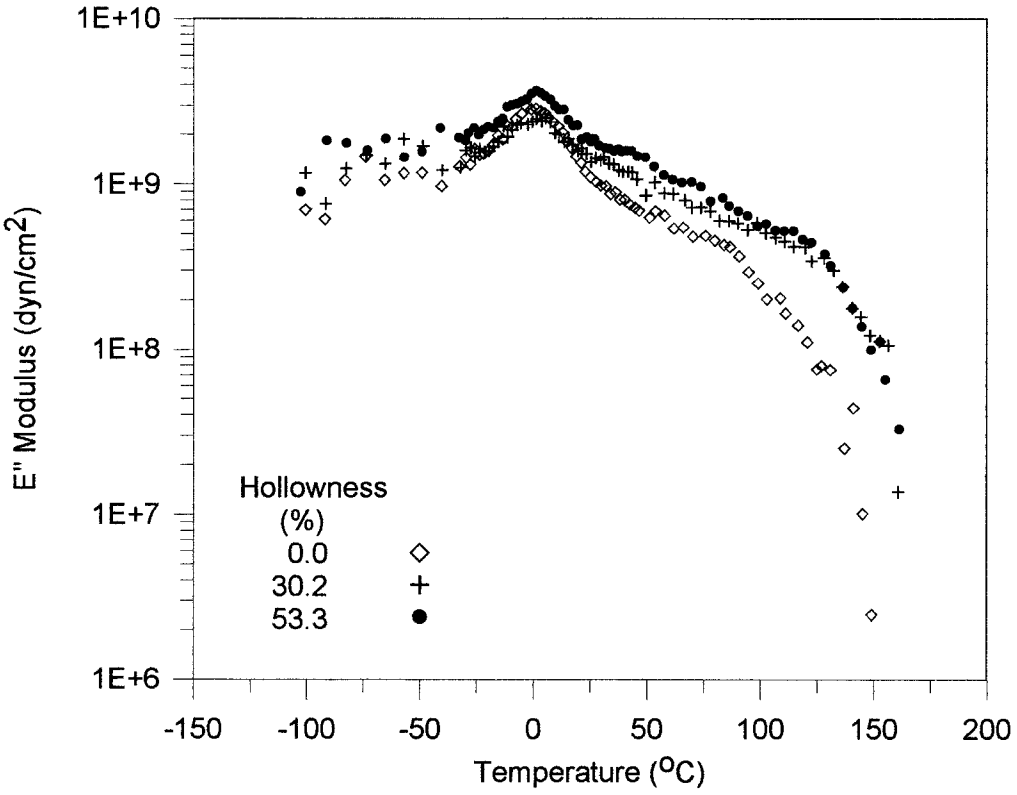

Figure 3 Loss modulus E'' as a function of temperature for fibers with constant cross-sectional area and various hollowness. Polymer throughput = 1.35 g/min; take-up speed = 840 m/min.

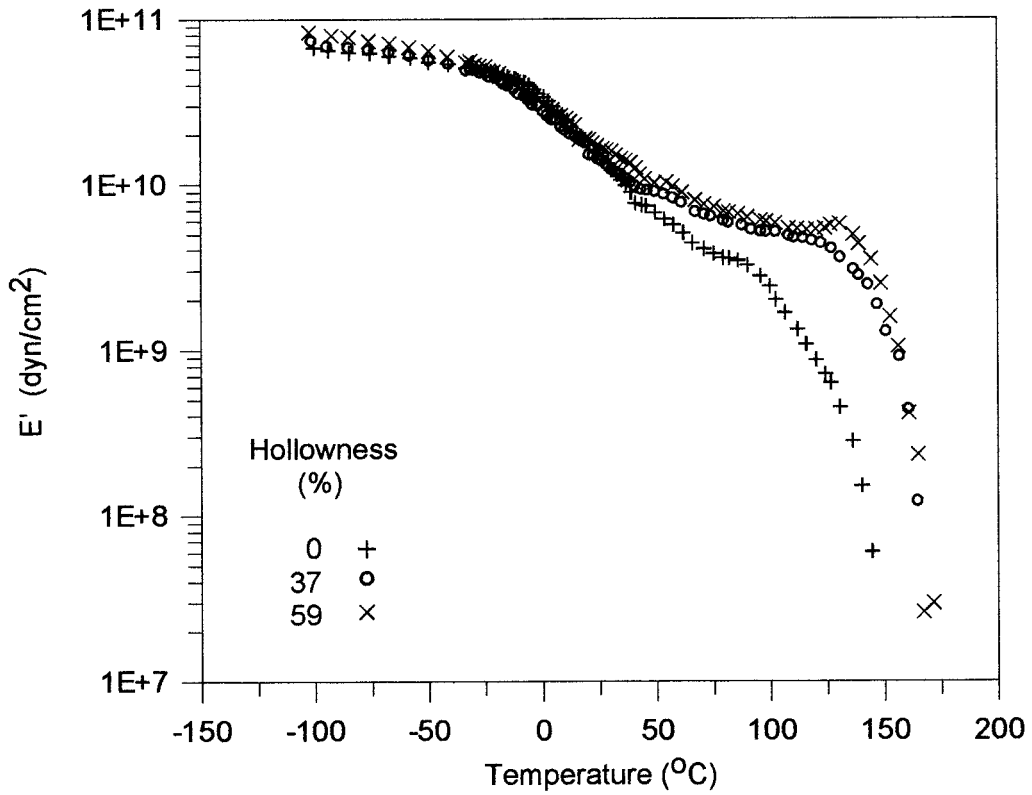

Figure 4 Storage modulus E' versus temperature for fibers with a constant outer diameter of 40 μm and various hollowness levels.

with an accuracy of ± 0.01 mg, and the samples were placed in an aluminum pan together with a drop of silicone oil to provide good thermal contact between sample and pan.[13] To test for possible unwanted side effects caused by the oil (e.g., plasticization), a solid fiber was immersed in silicone oil for 12 h. The diameter was measured before and after immersion, and no swelling was observed. Further, the silicone oil was carefully wiped off and the fiber tested using DMA. The elastic and the loss modulus curves before oil immersion were not different from the elastic and loss modulus curves after oil immersion. Thus, silicone oil does not measurably change fiber properties, and the oil can be safely used to improve the thermal contact during DSC experiments.

The melting temperatures quoted in this work are peak melting temperatures; that is, the temperatures corresponding to the maximum of the melting endotherm peaks. Crystallinity content of the fiber samples was determined using the commonly used relation[14]

$$\% \text{ crystallinity} = \frac{\Delta H_f}{\Delta H_0} \times 100 \qquad (3)$$

where ΔH_f is the heat of fusion of the sample and ΔH_0 is the heat of fusion of the same material with 100% crystallinity. A value of 146.5 J/g was assumed for ΔH_0.[15] The heat of fusion ΔH_f was determined by comparing the area under the sample melting endotherms to the area for fusion of indium samples. The commonly accepted indium heat of fusion is 6.802 cal/g.[16] The accuracy of the DSC measurements for melting temperature and crystallinity was estimated for both solid and hollow fibers. Three repeat experiments on solid fibers of 44 μm diameter were performed. These results were compared with those of three repeat experiments on hollow fibers with a 55.6 μm OD and 28.8 μm inner diameter (ID). The confidence interval, for a reliability of 0.95, was ± 1.5°C for T_m and $\pm 2\%$ for fractional crystallinity for both solid and hollow fiber samples. These low standard deviations show the excellent reproducibility of the sample preparation procedure.

RESULTS AND DISCUSSION

Effect of the Inner Diameter

To study the effect of the inner diameter, two different approaches were chosen. In the first ap-

Table III Fiber Properties at a Constant Outer Diameter of 40 μm

Hollowness (%)	Birefringence	T_g (°C)[a]	T_m (°C)[b]	Crystallinity (%)[b]	Spinning Speed (m/min)
0	0.00368	−0.3	161	39.6	592
37	0.00960	−10.0	164	55.7	1413
45	0.01500	−7.1	NA	NA	1665
59	0.01850	−7.2	164	44.5	1800
69	0.02690	−3.3	NA	NA	1800

[a] From dynamic mechanical analysis measurements.
[b] From differential scanning calorimetry measurements.

proach, we considered the effect of inside diameter with a constant polymer cross-sectional area (S_p was constant). In the second approach, we considered the effect of inside diameter with a constant outside diameter (S_f was constant).

Constant S_p

Fibers with a constant polymer cross-sectional area were experimentally obtained by spinning fibers at constant polymer throughput and constant take-up velocity. As mass neither enters nor leaves the spinline during the melt spinning of a fiber, the mass throughput at the exit of the spinneret is equal to the mass throughput at the collection roll. The mass conservation equation can be written as

$$m_p = \rho_p v S_p \tag{4}$$

where m_p is polymer mass throughput, ρ_p is polymer density; v is fiber velocity, and S_p is polymer cross-sectional area. The polymer throughput and spinning speed were kept constant at, respectively, 1.35 g/min and 840 m/min. Also, the polymer den-

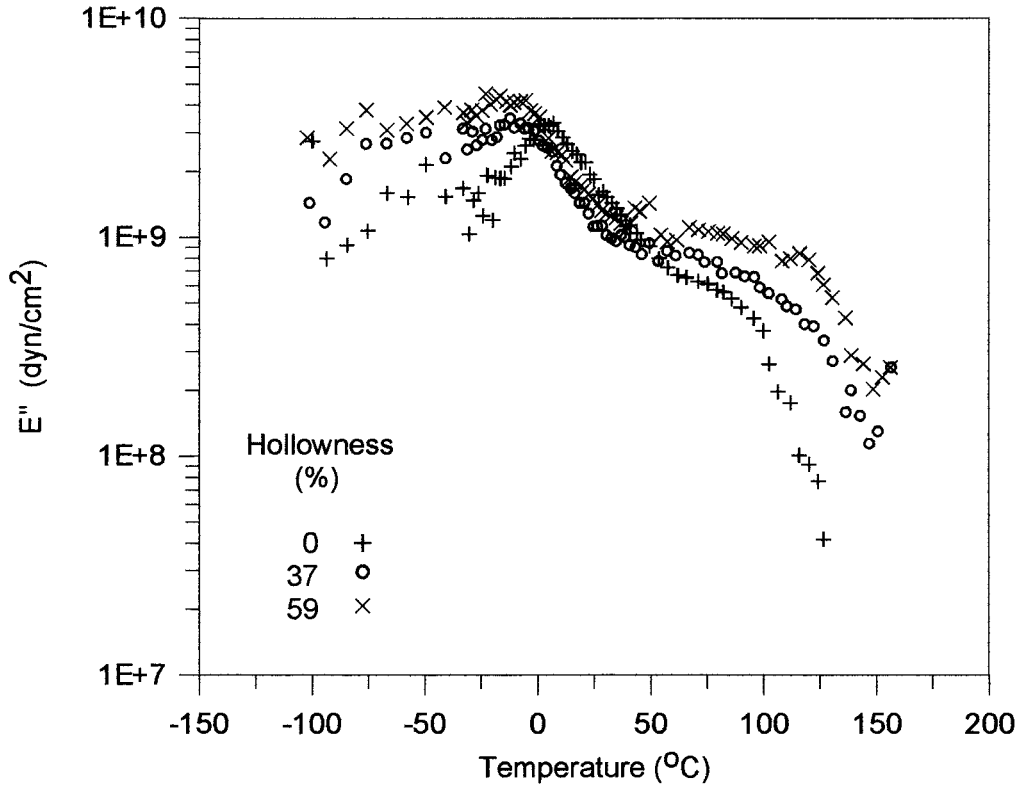

Figure 5 Loss modulus E'' versus temperature for fibers with constant outer diameter (40 μm) and various hollowness levels.

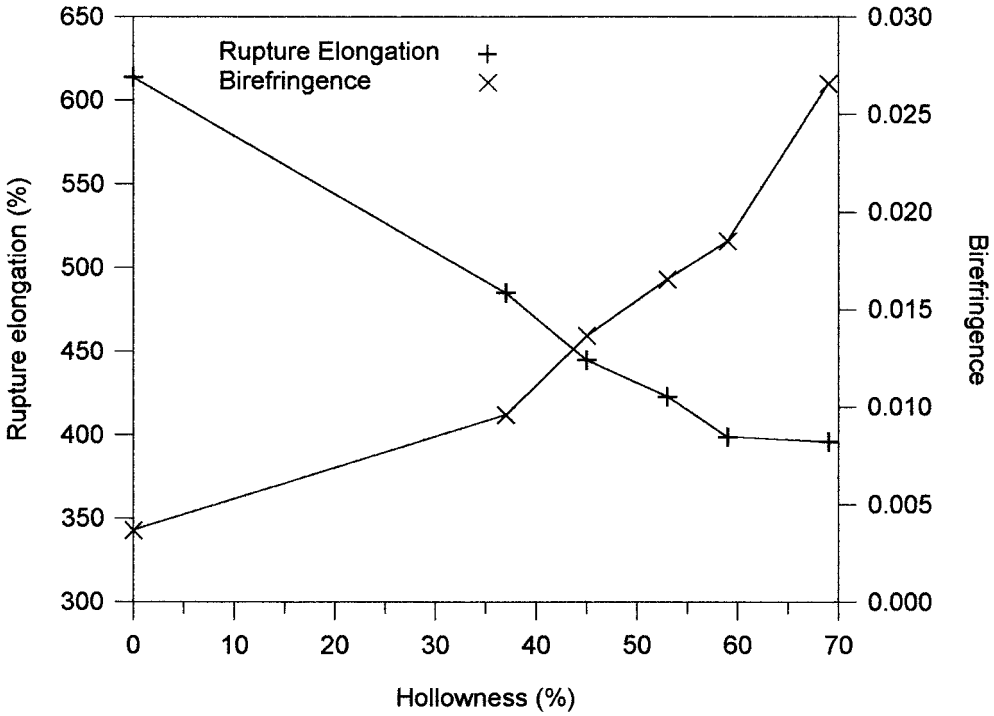

Figure 6 Rupture elongation and birefringence versus hollowness for fibers with a constant outer diameter of 40 microns.

sity was assumed to be a constant 0.895 g/cm^3.[8] Hence, as can be seen in Equation (4), the polymer cross-sectional area also stayed constant. The inner diameter was increased by increasing the flow of nitrogen injected into the core of the molten filament. The percentage void in the cross section is termed the hollowness, h, and is defined as

$$h = \left(\frac{\mathrm{ID}}{\mathrm{OD}}\right)^2 \tag{5}$$

This variable represents the ratio of the area of the hole to the total area of the fiber.

Figure 2 shows the variation of the storage modulus E' versus temperature for solid and hollow fibers spun with a polymer throughput of 1.35 g/min and a take-up speed of 840 m/min. The ID was varied to obtain a range of hollowness from 0 to 53.3%. According to both DSC and DMA (see Table II), hollow fibers showed a higher melting temperature when compared with the solid fiber, but little difference was found between the two hollow fibers. The increase in T_m indicates a larger crystal thickness for the hollow fibers, whereas an increase in fractional crystallinity in the hollow fibers is reflected in the increased modulus above the glass transition. A significant increase in modulus for the fiber with 53.3% hollowness was found versus that for the fiber with 30.2% hollowness. As the fractional crystallinities of these two samples were approximately identical, the increase in modulus is a reflection of the increase in orientation determined via birefringence (see Table II).

Figure 3 shows that no significant differences in glass transition temperature were found for any of the three samples. In contrast, most investigators have found that T_g increases as the fractional crystallinity increases; see Rabek[17] and Ziabicki.[18] Glass transition temperatures for solid and hollow fibers were equivalent probably because of higher orientation in the amorphous regions for the former; this orientation would offset the increase in T_g caused by a higher crystalline fraction in the hollow fibers.

Other researchers have both theoretically and experimentally studied crystallization in melt-spun fibers. Results from various experiments indicate that the structures formed during the process are caused by nonisothermal crystallization under molecular orientation.[19] In melt spinning, the fiber cools because of convective transfer with the ambient fluid (the air). This loss of heat is proportional to that of the outside area of the fiber. When spinning hollow and solid fibers with the same polymer cross-sectional area (i.e., con-

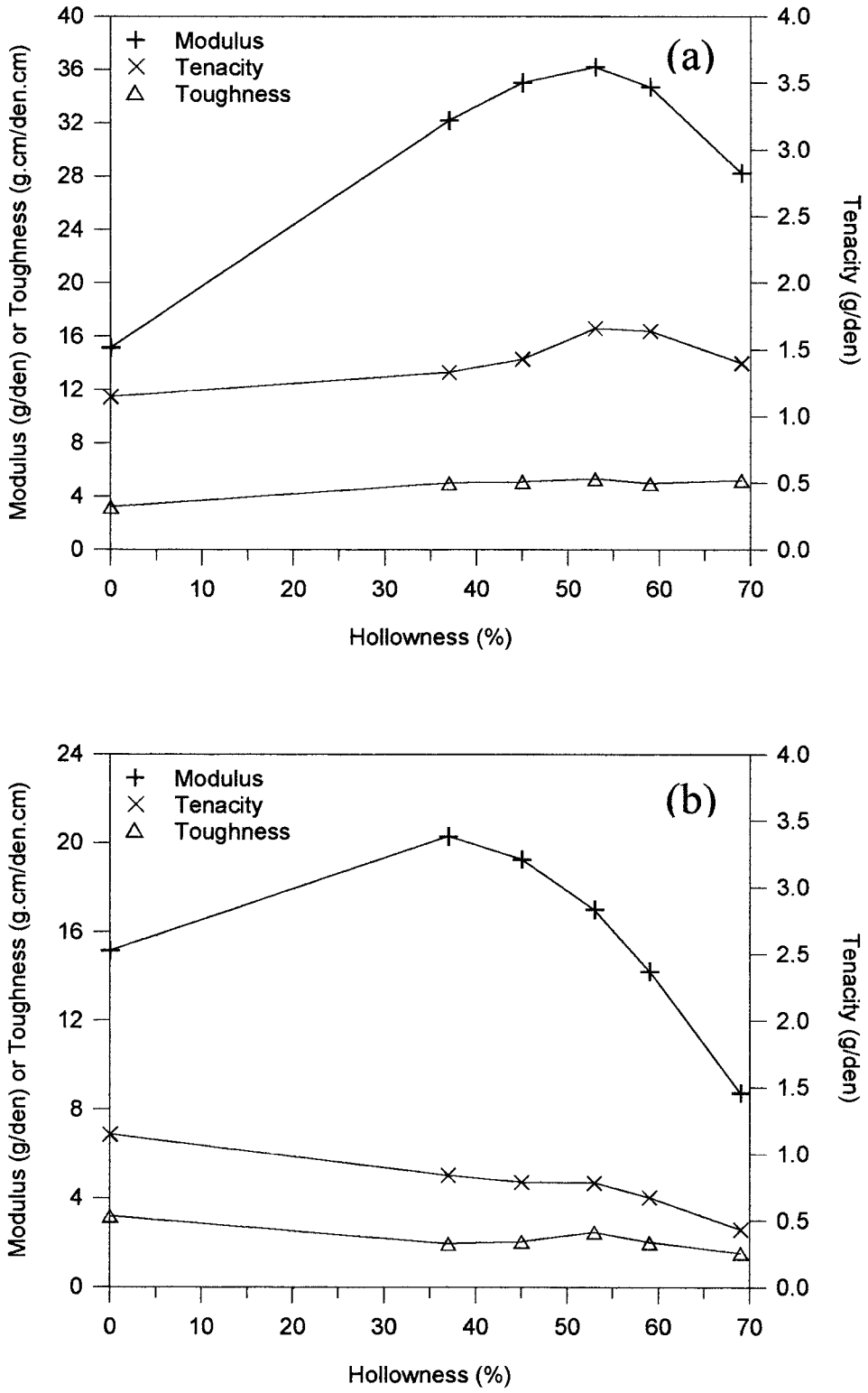

Figure 7 (a) Modulus, toughness, and tenacity versus hollowness for fibers with a constant outer diameter of 40 microns; all values were calculated based on polymer area, S_p. (b) Modulus, toughness, and tenacity for fibers with a constant outer diameter of 40 microns; all values were calculated based on the total fiber area, S_f.

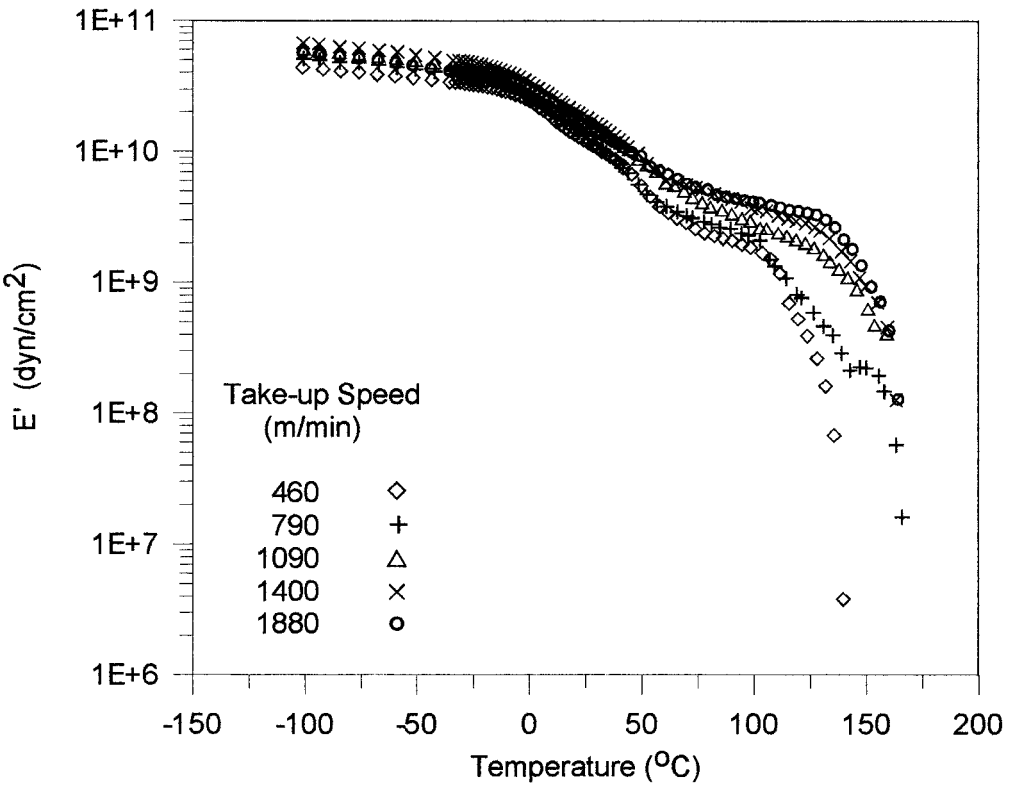

Figure 8 Storage modulus E' versus temperature for various spinning speeds. Polymer throughput = 2.33 g/min; nitrogen flowrate = 1.7 mL/min.

stant S_p), the hollow fibers have a larger outer diameter than the solid fibers. The larger outside diameter provides more cooling area for a hollow fiber; hence, hollow fibers are quenched faster than solid fibers, and this quick quenching leads to higher chain orientation. Higher orientation would induce higher crystallinity, and so orientation and crystallinity move in the same direction. However, stress development is different in hollow fibers versus solid fibers, and stress-induced crystallization can significantly affect the amount of crystalline material in the fiber.

Constant S_f

The effect of inner diameter was also studied while maintaining the OD constant. Various IDs were obtained using different combinations of polymer throughput, take-up speed, and nitrogen flowrate. Keeping OD constant is particularly interesting if one is considering replacement of solid fibers by hollow fibers, as replacement would probably require a fiber with the same outer diameter.

Figure 4 shows the effect of temperature on storage modulus E' for fibers with a constant OD and various IDs. Both DMA and DSC results show that no significant difference in T_m was observed between the 37% and 59% hollow fibers (Table III). The larger T_m in the hollow fibers is presumably indicative of a larger crystallite long spacing in the hollow fibers. The 37% hollowness fiber has a higher modulus than the solid fiber; this higher modulus corresponds to higher fiber crystallinity (see Table III). The modulus increased slightly as the hollowness increased from 37 to 59%. However, the crystallite fraction actually decreased as the hollowness increased. The increase of molecular orientation with increasing hollowness probably compensated for the drop of fractional crystallinity and explains the slight increase of modulus between the two hollow fibers. The increase of orientation with increasing hollowness was probably caused by faster quenching. Faster quenching was caused by lower polymer throughput with increased hollowness (i.e., less material to cool).

Figure 5 shows, for a constant outside diameter, the loss modulus E'' for a solid fiber and two hollow fibers. The variation of the glass transition temperature with hollowness was very complex.

Table IV Fiber Properties at Various Spinning Speeds[a]

Take-up Speed (m/min)	T_g (°C)[b]	T_m (°C)[c]	Crystallinity (%)[c]	Birefringence
460	5.0	162.6	26.4	0.00563
790	5.0	162.6	36.2	0.00770
1090	2.2	163.8	59.8	0.01000
1400	0.5	163.5	50.3	0.01230
1880	−10.0	163.1	37.1	0.01440

[a] The polymer throughput was 2.33 g/min and the nitrogen flowrate was 1.7 ml/min.
[b] From dynamic mechanical analysis measurements.
[c] From differential scanning calorimetry measurements.

The T_g of the 37% hollow fiber is actually less than the T_g of the solid fiber, even though, as shown in Table III, fractional crystallinity is higher in the 37% hollow fiber. Once again, we assign this counterintuitive observation to higher amorphous chain orientation in the solid fiber. The increase of T_g between 37 and 59% hollowness could be explained by the decrease of fractional crystallinity. The reduced fractional crystallinity would allow higher amorphous orientation in the 59% hollow fiber.

Rupture elongation is defined as the elongation where the sample breaks; our rupture tests were done on an Instron tensile tester (Instron, Inc., Canton, MA). Figure 6 shows rupture elongation versus hollowness for fibers with constant OD (40 μm). Birefringence (via polarized-light microscopy) is also shown. The same fibers used in the DMA tests were used for the tensile and birefringence tests. In addition, a fiber with 53% hollowness was tested. As expected, birefringence increased with increasing hollowness, whereas rup-

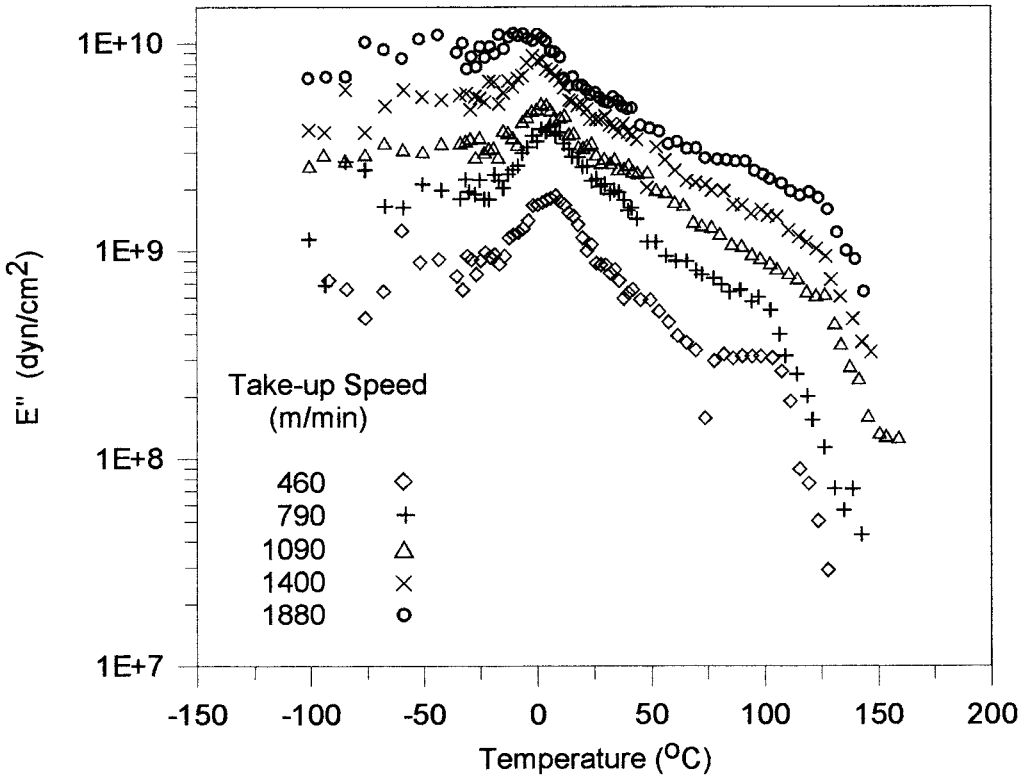

Figure 9 Loss modulus E'' versus temperature for various spinning speeds. Polymer throughput = 2.33 g/min; nitrogen flowrate = 1.7 mL/min.

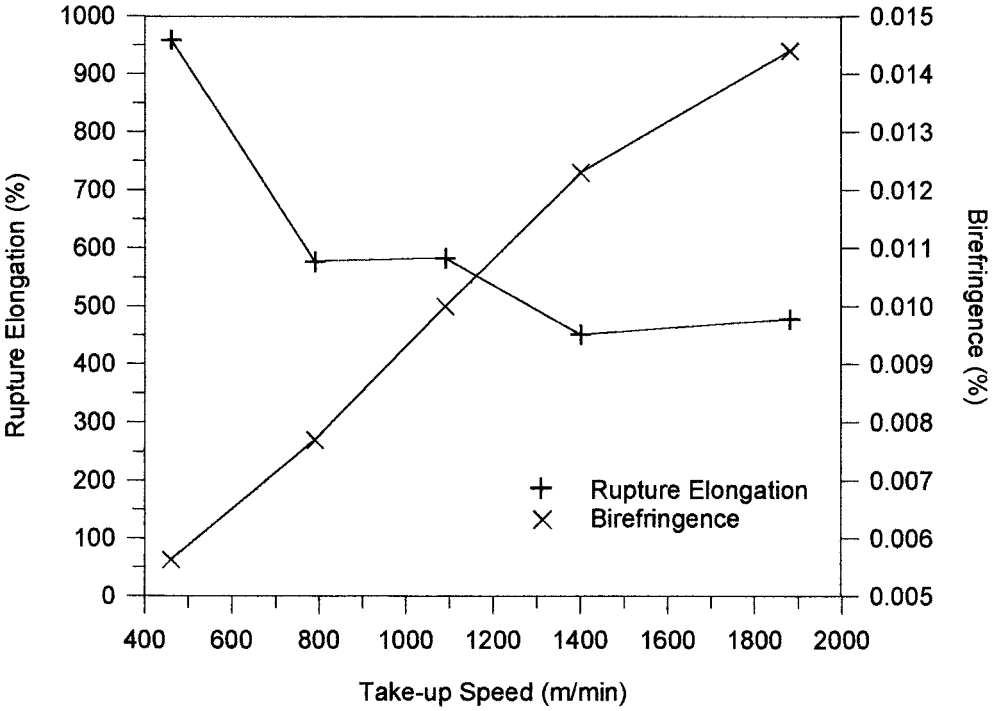

Figure 10 Effect of spinning speed on rupture elongation and birefringence for hollow fibers. Polymer throughput = 2.33 g/min; nitrogen flowrate = 1.7 mL/min.

ture elongation decreased. Rupture elongation and birefringence are actually closely connected because high orientation (which birefringence measures) limits the maximum elongation that can be reached. At a hollowness of 69%, the birefringence almost reached 0.03. This birefringence level is typical of full-strength, commercial polypropylene fibers.

Figure 7(a) shows modulus, tenacity, and toughness as functions of hollowness. The presence of hollowness had little effect on toughness, but a more complex effect on modulus and tenacity was observed. Both modulus and tenacity increased with increasing birefringence up to a hollowness of 50% (birefringence of ca. 0.015). After that point, modulus and tenacity decreased, whereas birefringence continued to increase.

Figure 7(b) shows the modulus, toughness, and tenacity for the same fibers as shown in Figure 7(a), but in Figure 7(b), the stress was calculated on the basis of the total fiber area, S_f, instead of the polymer area, S_p [as was done for Fig. 7(a)]. If hollow fibers are to replace solid fibers, the load on a per outer diameter basis, not a per polymer basis, will be the more relevant parameter. The modulus, even based on the outside diameter, clearly increases with increasing hollowness. It is shown in Figure 7(b) that half the polymer can be used to produce a fiber with the same modulus. [Keep in mind that, for Fig. 7(b), the modulus was calculated using the total fiber area, not the polymer area.] The tenacity and toughness drop slightly with increasing hollowness when compared on this basis; whether this drop is monotonic between 0 and 37% hollowness [as Figure 7(b) implies] is not known because data were not collected in this region.

Effect of Take-Up Velocity

Figure 8 shows the effect of spinning (take-up) speed on elastic modulus. Hollow fibers were spun at speeds of 460–1880 m/min. All fibers were produced with a polymer throughput of 2.33 g/min and a nitrogen flowrate of 1.7 mL/min. These fibers had identical hollowness (ca. 40%), as the ratio of inner to outer diameter is not a function of final take-up speed. On the basis of the nitrogen and polymer mass balance equations, hollowness can be calculated from the relation

$$\left(\frac{\mathrm{ID}}{\mathrm{OD}}\right)^2 = \frac{\dfrac{m_n}{\rho_n}}{\dfrac{m_n}{\rho_n} + \dfrac{m_p}{\rho_p}} \tag{6}$$

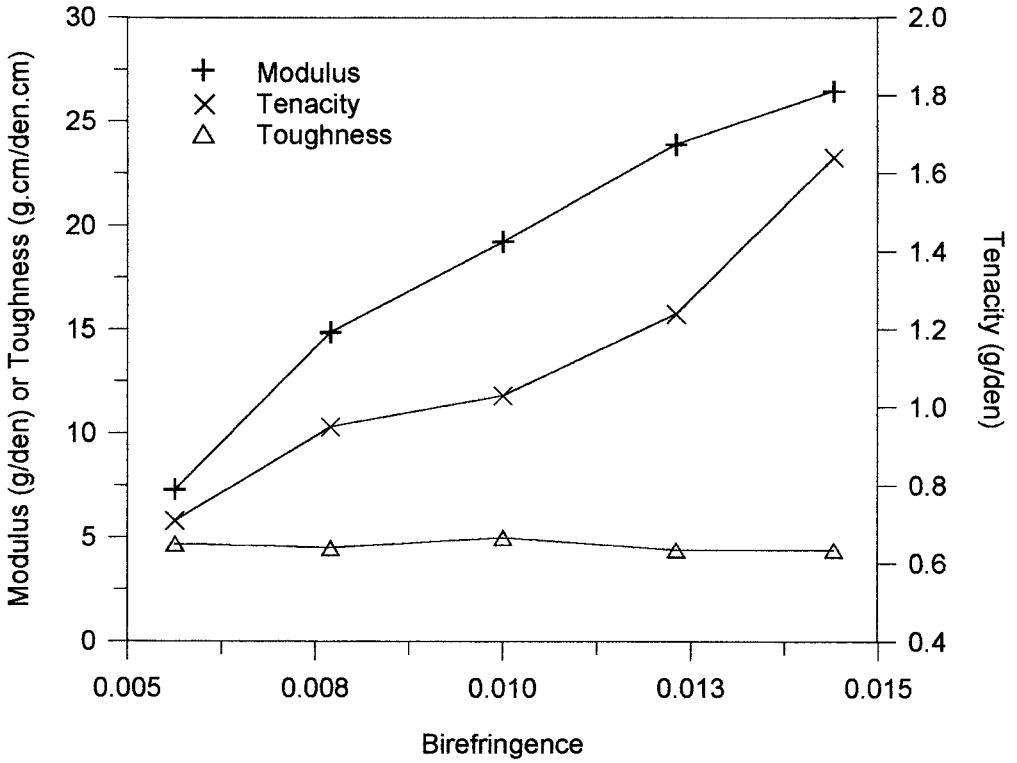

Figure 11 Effect of spinning speed on modulus, toughness, and tenacity for hollow fibers. Polymer throughput = 2.33 g/min; nitrogen flowrate = 1.7 mL/min.

where m_p is polymer mass throughput, m_n is nitrogen mass flowrate, ρ_p is polymer density, and ρ_n is nitrogen density.

In Figure 8, hollow fibers spun with increasing take-up speed show increasing modulus at ambient temperature. These results correlate with the data in Table IV: Both fractional crystallinity and molecular orientation (birefringence) increase as spinning speed increases up to 1400 m/min. For fibers spun at higher speeds (1400 and 1880 m/min), the fractional crystallinity starts to go down, but the molecular orientation and the modulus keep increasing. Hence, the increase of orientation was alone responsible for the higher moduli of the 1400 and 1880 m/min fibers. Drawing has been shown to decrease crystallinity.[20] Galanti and Mantell[20] showed that amorphous structures orient more rapidly than crystalline structures in fibers because amorphous structures have a greater mobility than crystallites. Moreover, the decrease in polymer cross-sectional area with the increase in spinning speed results in faster quenching, which could also reduce fractional crystallinity. Thus, the high drawing rates of 1400 and 1880 m/min may start limiting crystal growth by increasing the amount of oriented amorphous material in the fiber.

Figure 9 was produced with the same fibers used to develop Figure 8. However, Figure 9 shows the loss modulus. As spinning speed increases, the glass transition temperature dropped from 5°C at 460 m/min to –10°C at 1880 m/min (see Table IV). For final spinning speeds between 460 and 1090 m/min, the decrease in T_g was probably a tradeoff between a higher crystalline fraction and lower amorphous orientation. For higher speeds, Table IV shows that T_g decreases as fractional crystallinity decreases, as expected. As also shown in Table IV, spinning speed had very little effect on T_m; thus, spinning speed did not affect crystallite size.

The increase in orientation produced by drawing influences the mechanical properties of polypropylene filaments. Rupture elongation and birefringence are plotted versus take-up speed in Figure 10. As expected for higher spinning speeds, orientation increases and elongation at break decreases. Figure 11 represents the variation of modulus, toughness, and tenacity as a function of spinning speed. Toughness shows little variation, whereas modulus and tenacity increase as spinning speed increases. This observation is typical of solid fibers.[7] As described earlier, a maximum in fractional crystallinity of approxi-

mately 55% and a maximum in tenacity of approximately 1.5 g/den were found for constant OD and a birefringence and hollowness of 0.015 and 50%, respectively. The 55% crystallinity also represents the approximate maximum in fractional crystallinity for different spinning speeds, but the birefringence at this crystallinity is 0.01, a much lower value. Unlike when the hollowness changed, the tenacity did not reach any limit as the spinning speed changed, perhaps because the birefringence was not as high.

CONCLUSIONS

The mechanical and thermal properties of hollow fibers were compared with the properties of solid fibers. Hollow fibers exhibited greater crystallinity, orientation, modulus, and tenacity, regardless of whether the outer diameter or the hollowness are kept constant. Up to a hollowness level of about 50%, a larger inner diameter and higher spinning speeds increase fiber properties. Crystallinity reached a maximum of about 55–60% at intermediate take-up speeds and at intermediate hollowness.

By introducing another processing variable—nitrogen flow through the center of the die—fibers were produced outside the normal property envelope of melt spun solid fibers. Producing a hole in the center of the fiber changed the balance between orientation and crystallinity. Quantitatively, our results show that a fiber with 55% of the weight [determined from Figure 7(b)] of a solid fiber at the same cross-sectional area would have the same modulus as a solid fiber. This result is only for one type of polymer at one outer diameter, but it is likely that similar types of improvements would be found with other polymers at other outer diameters.

REFERENCES

1. Baum, B.; Holley, Jr., W.; White, R. A. In Membrane Separation Processes; Meares, P. Ed.; Elsevier Scientific: New York, 1976.
2. Kim, J. J.; Jang, T. S.; Kwong, Y. D.; Kim, U. Y.; Kim, S. S. J Membrane Sci 1994, 93, 209.
3. Kim, J. H.; Park, Y.I.; Jegal, J.; Lee, K.H. J Appl Polym Sci 1995, 57, 1637.
4. Capiati, N. M.; Porter, R. S. J Polym Sci Polym Phys 1975, 13, 1177.
5. Kim, J. J.; Hwang, J. R.; Kim, U. Y.; Kim, S. S. J Membrane Sci 1995, 108, 25.
6. Moch, I. In Encyclopedia of Chemical Technology, 4th ed.; 1991; Vol. 13.
7. Ahmed, M. Polypropylene Fibers—Science and Technology; Elsevier Scientific: New York, 1982.
8. Bansal, V.; Shambaugh, R. L. Polym Eng. Sci. 1996, 36, 2785.
9. Khanna, Y. P.; Wenner, W. M.; Kumar, R.; Kavesh, S. J Appl Polym Sci 1989, 38, 571.
10. Khanna, Y. P.; Taylor, T. J.; Kumar, R. J Appl Polym Sci 1991, 42, 693.
11. Gander, R.; Schaefer, A. Microskopion 1968, 15, 2.
12. Bershtein, V. A.; Egorov, V. M. Differential Scanning Calorimetry of Polymers; Ellis Horwood: New York, 1994.
13. Smook, J.; Pennings, J. Colloid Polym Sci 1984, 262, 712.
14. Dole, M. J Polymer Sci. 1967, 18, 57.
15. Huda, M. N.; Dragaun, H.; Bauer, S.; Muschik, H.; Skalicky, P. Colloid Polym Sci 1985, 263, 730.
16. Dean, J. A. Lange's Handbook of Chemistry, 11th ed.; McGraw-Hill: New York, 1973.
17. Rabek, J. F. Experimental Methods in Polymer Chemistry; Wiley: New York, 1980; p 534.
18. Ziabicki, A. Fundamentals of Fibre Formation; Wiley: New York, 1976.
19. Jinan, C.; Kikutani, T.; Takaku, A.; Shimizu, J. J Appl Polymer Sci 1989, 37, 2683.
20. Galanti, A. V.; Mantell, C. L. Polypropylene Fibers and Films; Plenum: New York, 1965.